



# Projecting Climate Change Effect on Soil Water Fluxes and Urea Fertilizer Fate in the Semiarid Pampas of Argentina

Leonardo E. Scherger<sup>1,2</sup> · Javier Valdes-Abellan<sup>3</sup> · Victoria Zanello<sup>1,2</sup> · Claudio Lexow<sup>2</sup>

Received: 21 September 2021 / Revised: 17 December 2021 / Accepted: 18 December 2021  
© King Abdulaziz University and Springer Nature Switzerland AG 2022

## Abstract

The economy of the semiarid region of the Argentine Pampas is based mainly on agriculture, so climate change is a fact that may have great influence on this type of activity. Therefore, it is necessary to evaluate future climate scenarios and the responses of hydrological variables such as precipitation, actual ( $ET_{real}$ ) and potential evapotranspiration ( $ET_c$ ), and recharge rate. Climate change scenarios were based on temperature and precipitation variations predicted by CMIP5. Four representative concentrations pathways (RCP) were considered according to different greenhouse emissions to the atmosphere for the nearby future until the end of the twenty-first century (RCP2.6, RCP4.5, RCP6.0 and RCP8.5). Furthermore, one more scenario called RCP0.0 was considered, which is related to the actual climate conditions and represents the base line. In the study area, nitrogen (N) fertilization is a widely used practice to increase crop yields. This work assesses the impact of future climate on soil water fluxes and N compounds fate based on numerical simulations carried out with HYDRUS 1D. Actual evapotranspiration is going to increase between 1 and 6% from low to high climate-change scenarios. Although an increase in precipitation is also expected during all months of the year, there are periods when water availability will not be enough to supply the new potential evapotranspiration demand. The worst case is RCP8.5, where the  $ET_{real}/ET_c$  ratio is expected to decline by 4%. Annual recharge is expected to decrease by 2.5% in the RCP2.6 scenario, while the rest of the scenarios shown positive trends. N leachate in the form of nitrates showed an increase of 2.8% in the RCP4.5 scenario which was also the one with the highest recharge rate raise. The use of a mathematical model as a predictive tool in soil water fluxes and fertilizers use is essential for planning the sustainable management of agroecology adapted to climate changes.

**Keywords** Climate change · Weather generator · Nitrogen compounds fate · Argentine Pampas · HYDRUS 1D

## 1 Introduction

Global climate change is a key research topic, as it will have a direct impact on crop production, natural hazards frequency, air temperature increase, soil degradation by nutrients leachate and decrease in freshwater availability (Rao et al. 2016). According to the IPCC (2014) the global surface temperature is projected to increase by 3.7° C by the end of the twenty-first century. In addition, the intensity of

climate conditions is expected to be more extreme, increasing the severity of droughts and floods.

Climate change will undoubtedly affect agriculture (Abera et al. 2018) and the sustainability of agriculture systems needs to be addressed for each particular situation. Regional climate changes have a direct impact on agricultural and livestock production (Ghahramani and Moore 2016; Henry et al. 2018), with serious consequences for social-ecological sustainability and food security (Almazroui et al. 2021). This may be the case of the semiarid region of Argentine Pampas, where water resources are very sensitive to climate variability. Since the 1960s an increase in crop yields in the Pampas region has been observed, fostered by both technology and climate trends. The increase in spring and summer rainfall observed in several regions of Argentina, favored annual crops productivity and the inclusion of new lands for agriculture (Barros et al. 2015). Barros et al. (2000) indicated a total annual precipitation increase of

✉ Leonardo E. Scherger  
leonardo.scherger@uns.edu.ar

<sup>1</sup> Consejo Nacional de Investigaciones Científicas y Técnicas (CONICET), CCT Bahía Blanca, Bahía Blanca, Argentina

<sup>2</sup> Departamento de Geología, Universidad Nacional del Sur (UNS), Av. Alem 1253, 8000 Bahía Blanca, Argentina

<sup>3</sup> Departamento de Ingeniería Civil, Universidad de Alicante (UA), Alicante, España

about 30% between 1956 and 1991 for the central and eastern Argentine region. This climate changes favor an important agricultural expansion over semiarid steppes (Barros et al. 2008). However, severe drought had also affected this region during the last century, having serious impacts on crop production (Podestá et al. 2009; Abraham et al. 2016). For the reasons listed above, the semiarid pampas are sensitive to climatic fluctuations, so it is necessary to evaluate the impact of future climate change over soil water fluxes.

Nitrogen (N) fertilization is an important management practice to increased grain yield (Barbieri et al. 2008). In the south Pampas intensive cropping with conventional tillage has led to a deterioration of soil fertility. A reduction in soil organic matter increased soil erosion and exacerbated N deficiency problems (Studdert and Echeverría 2000). Nowadays, soil capacity to sustain abundant crop production is artificially maintained by external fertilization to restore nutrient levels (Carbonetto et al. 2014). However, when excessive N input exceeds crop demand, N could be loss to the environment via multiple pathways. Ammonia ( $\text{N-NH}_3$ ) volatilization is one of the major N losses from soil fertilization. The worldwide losses present an average value of 14% (range from 10 to 19%) of the used N fertilizers (Ferm 1998). Fertilizer losses is not only an economical problem, also the release of nitrate ( $\text{N-NO}_3$ ) to the environment is considered the most problematic pollutant in intensive agricultural production areas (Zupanc et al. 2011). Due to its mobility in the soil, nitrate leaching can occur at and after harvest as well as during the crop cycle because of excessive irrigation or heavy precipitation (Saadi and Maslouhí 2003; Zhou et al. 2006; Phogat et al. 2014). According to world databases nitrate N lost by leaching is assumed to be 30% of applied fertilizer N (Wang et al. 2019). Fertilizer inputs are considered one of the major concerns in the environmental impact of agronomical systems. Climatic conditions will regulate soil water flows, but also the fate of N compounds derived from fertilizers.

Several climate models were developed to predict the climate change. Those models are developed at a global scale from general circulation models (GCMs) or at a regional scale by dynamical downscaling of GCMs obtaining regional climate models (RCMs) (Cabré et al. 2016). The IPCC have made available a set of climate simulations and scenarios that is known as Couple Model Intercomparison Project Phase 5 (CMIP5) (Kharin et al. 2013). The CMIP5 depends on several global and/or regional climate models from research institutes worldwide. CMIP5 is based on more sophisticated climate models and a new suite of forcing scenarios compared to its predecessor CMIP3. Four different representative concentration pathways (RCPs) (IPCC 2013), have been defined according to four different concentration levels of greenhouse gases emissions. The IPCC assesses climate change according to the future development of

mankind along with the associated environmental and socio-economic impacts.

Numerical models are an efficient tool to predict water fluxes and solute transport in soil (Akbariyeh et al. 2018). The HYDRUS code (Šimůnek et al. 2013) has proven its applicability in a myriad of research studies. Several works have tested the code capacity to represent N compounds transport in soil (Hanson et al. 2006; Phogat et al. 2014; Li et al. 2015; Iqbal et al. 2016; Karandish and Šimůnek 2017). The HYDRUS code has also been applied in projecting climate-change effect over soil water fluxes and solute transport. Wang et al. (2021) studied climate-change effects on soil water dynamics of maize in Chinese croplands. Similarly, Ferreira et al. (2021) evaluated climate and soil water variations in corn crops. Haj-Amor and Bouri (2020) evaluated the effects of future climate on soil salinization. Morales et al. (2016) applied HYDRUS software to simulate the fate and transport of N under actual and changing climate scenarios.

In this work, we evaluate the impact of climate change on soil water fluxes and the fate of N compounds derived from the most used synthetic fertilizer, urea (46% N). For this purpose, a synthetic climate series was developed by a stochastic weather generator for the semiarid region of the Argentine Pampas. Then, five climate scenarios based on IPCC predictions for different RCPs were considered and the HYDRUS software was applied to simulate vadose zone fluxes for a period of 100 years. Knowing the evolution of soil water content and the fate of N under future climates will be fundamental for planning the development of a sustainable agriculture, both in economic and environmental terms.

## 2 Material and Methods

### 2.1 Study Area and Soil Properties

The study area is located within the southwestern region of Buenos Aires Province ( $38^\circ\text{--}40^\circ\text{ S}$ ;  $60^\circ\text{--}62^\circ\text{ W}$ ), Argentina (Fig. 1). According to the world climate classification of Köppen–Geiger, the region is a transition between the sub-humid temperate climate of the Pampas plain and the semi-arid climate of Argentine Patagonia. The annual mean temperature is  $15.3^\circ\text{ C}$  (maximum annual mean temperature of  $22.1^\circ\text{ C}$  and minimum annual mean temperature of  $8.5^\circ\text{ C}$ ) and the annual mean rainfall is 593 mm (series 1956–2020). Maximum rainfall occurs in spring and autumn. Meanwhile, winter and summer are the driest seasons (Scherger et al. 2021). In the region, cereal crops (mainly wheat and barley) are usually grown continuously during winter, in rotation with sunflower or with a year-long fallow in between crops (Schmidt et al. 2018). Additionally, several forages and

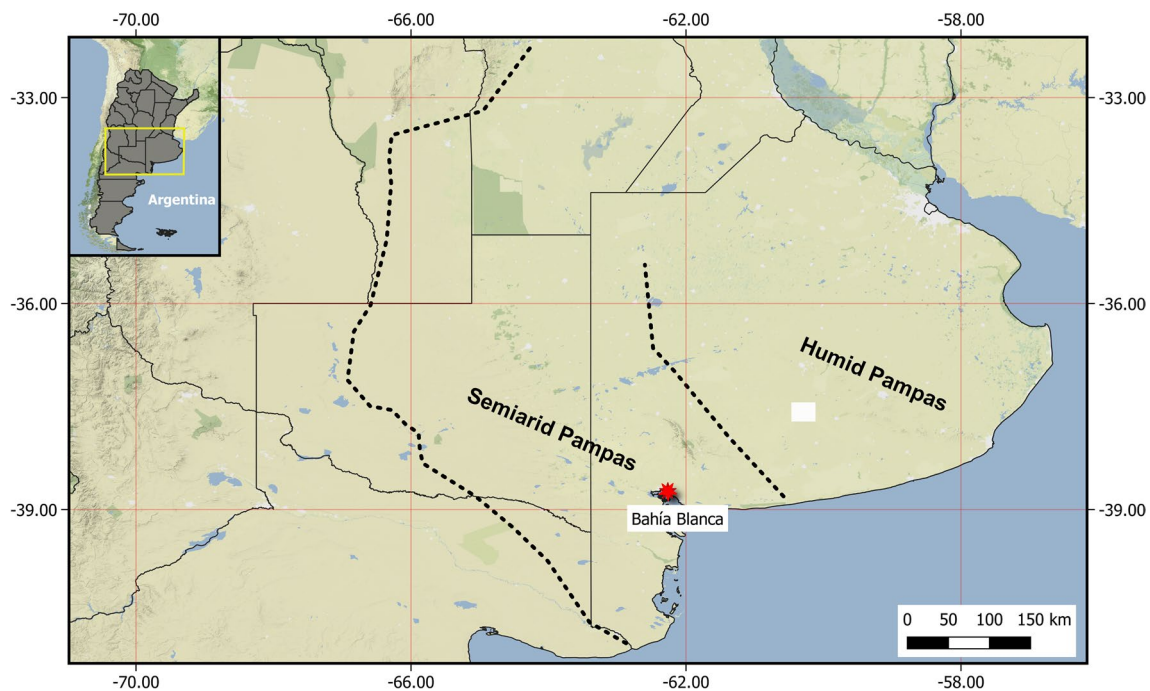


**Fig. 1** Location map of the study area

grazing pastures are cropped to feed livestock. The forage crops (e.g. oats, corn, sorghum, and rye) are cultivated under conventional tillage. Rotation pasture composed mainly of alfalfa and gramineous plants are followed by four or more years of grain crops (Quiroga et al. 1999). In all cases, crop yields are limited by water availability.

Most soils of the Pampas were developed from *loess* deposits and are mainly Mollisols (Rimski-Korsakov et al. 2015). Particularly, in the study region the dominant soils classified as Petrocalcic Paleustolls, Entic Haplustolls and Typic Haplustolls (Díaz-Zorita et al. 2002; Noellemeyer et al. 2006; Schmidt et al. 2018). In the region, soils have suffered erosive process by long-term exposure to intense winds and led to coarse textures of the surface horizons (Amiotti et al. 2001). The dominant texture is sandy loam coexisting alongside other soils that preserve *loess* original finer textures.

## 2.2 Climate Change Scenarios

The IPCC (2013) in its assessment report included the atlas of global and regional climate forecast for seasonal precipitation and temperature changes from 70 regions of the Earth. The predicted climate changes were calculated using a set of global and/or regional models called CMIP5. In this study, four representative concentrations pathways (RCP) established by the IPCC (i.e., RCP2.6, RCP4.5, RCP6.0 and RCP8.5) were considered to evaluate climate-change scenarios. These RCPs established different greenhouse

emissions to the atmosphere for the nearby future until the end of the twenty-first century. RCP2.6 comprises the lowest emissions scenario, and it considers an increase of  $2.6 \text{ W m}^{-2}$  in the radiative forcing. RCP4.5 and RCP6.0 are the two intermedium emissions scenarios, predicting a radiative forcing increase of  $4.5$  and  $6.0 \text{ W m}^{-2}$ , respectively. The highest emissions scenarios (RCP8.5) considers an increase of  $8.5 \text{ W m}^{-2}$ . Not adopting any measure to reduce the emissions of greenhouse will led to situation between scenarios RCP6.0 and RCP8.5 (Greve et al. 2018). Following the strategy of other studies (Valdes-Abellan et al. (2020)), a fifth scenario called RCP0.0 was also considered, which its related to the actual climate conditions and represents the base line of the study area. The climate-change predictions evaluated in this study corresponds with the 50th percentile of the temperature and precipitation variations projected by CMIP5 for the southeastern South America region (Table 1).

## 2.3 Climatic Series Generation

The meteorological data used in the study were obtained from the AERO-Bahía Blanca weather station ( $38^{\circ} 43' 3.15'' \text{ S}$ ,  $62^{\circ} 9' 55.81'' \text{ W}$ ), supported by the Argentinian National Meteorological Service. Meteorological data on a daily scale were available for the period 1956–2020 (64 years). These data were used to produce synthetic series for the study area of daily precipitation, minimum and maximum air temperature, by the weather generator CLIGEN (Nicks et al. 1995). CLIGEN generates, besides the previous ones, a set

**Table 1** Temperature (°C) and precipitation (%) variations for each climate-change scenario for the southeastern South America region according to the IPCC (2013) and 50th percentile of the CMIP5

	Temperature (°C)				Precipitation (%)	
	Dec–Jan–Feb	Mar–Apr–May	Jun–Jul–Aug	Sep–Oct–Nov	Oct–Mar	Apr–Sep
RCP2.6	0.8250	0.792	0.7788	0.8644	0.830	0.420
RCP4.5	1.6925	1.6549	1.4856	1.5936	3.720	4.240
RCP6.0	2.0580	2.0832	1.6850	1.9949	3.840	3.680
RCP8.5	3.7735	3.6174	3.4324	3.7916	5.730	7.060

of different meteorological variables such as radiation, wind velocity or dew temperature. All variables are generated at a daily scale. CLIGEN demands a complete set of statistical data to correctly produce synthetic data, statistically equal to the observed climate. Among the required statistics by CLIGEN there is the mean, standard deviation, and skewness for precipitation at a monthly scale, the probabilities of a wet day after a wet day and a dry day after a wet day, the minimum and maximum values of air temperature were incorporated as the mean and standard deviation for each month of the year.

A synthetic weather series of 1000-year was created, which represents the actual climate conditions and was assigned to the RCP0.0 scenario. Meanwhile, the 1000-year synthetic series was modified according to temperature and precipitation variation from Table 1, and represent the climate-change scenarios RCP2.6, RCP4.5, RCP6.0 and RCP8.5, respectively. Random 100-year series were obtained from it to reproduce the different scenarios.

## 2.4 Numerical Model

The HYDRUS 1D code (Šimůnek et al. 2013) was applied to simulate urea transport in the soil under different climate conditions. The software is a mathematical code, which allows the resolution of the modified Richards equation for unsaturated water flow and convection–dispersion equation for solute transport. HYDRUS 1D allows the simulation of multiple solutes subject to first-order decay reactions, such as nitrogen

### 2.4.1 Water Flow

One-dimensional unsaturated water flow was simulated according to the modified Richards equation:

$$\frac{\partial \theta}{\partial t} = \frac{\partial}{\partial z} \left[ K(h) \frac{\partial h}{\partial z} \right] - S,$$

where  $\theta$  is the volumetric water content (–),  $h$  is the pressure head (L),  $t$  is time (T),  $z$  is the vertical position (L),  $S$  is a sink term that represent the water extraction by roots ( $T^{-1}$ ) and  $K(h)$  is the unsaturated hydraulic conductivity ( $LT^{-1}$ ). The

hydraulic model was proposed by van Genuchten–Mualem (van Genuchten 1980):

$$S_e = \frac{\theta(h) - \theta_r}{\theta_s - \theta_r} = [1 + (\alpha h)^n]^{-m}$$

$$K(h) = K_s S_e^l \left[ 1 - (1 - S_e^{\frac{1}{m}})^m \right]^2,$$

where  $S_e$  is the effective humidity,  $\theta_r$  and  $\theta_s$  (–) are the residual and saturated water contents respectively,  $\alpha$  ( $L^{-1}$ ) is related to the inverse of the air-entry suction ( $h_a$ ),  $n$  and  $m$  (–) are empirical parameters dependent on soil properties, where  $m = 1 - 1/n^{-1}$ , and  $l$  (–) is the pore conductivity, which has a value of 0.5 as an average of different soils (Mualem 1976).

The root water uptake model was described by Feddes et al. (1974):

$$S = \alpha(h) S_p,$$

where  $\alpha(h)$  is a dimensionless water stress response function ( $0 \leq \alpha \leq 1$ ) and  $S_p$  is the potential water uptake. Root water uptake is null under or near soil saturation ( $h_1$ ) or under greater pressure heads than the wilting point ( $h_4$ ). Transpiration rate is maximum as  $\alpha$  equals 1 when  $h_2 < h < h_3$ . For the ranges of  $h_4 < h < h_3$  and  $h_2 < h < h_1$ , transpiration decrease linearly as the pressure head decrease or increase, respectively. The values for the current crop were taken from Wesseling (1991) for pastures ( $h_1 = -10$  cm;  $h_2 = 25$  cm;  $h_{3,1} = -200$  cm;  $h_{3,2} = -800$  cm; and  $h_4 = -8000$  cm). The maximum rooting depth was assumed as 80 cm.

### 2.4.2 Solute Transport

Urea degradation can be expressed in a sequential first-order decay chain as (Šimůnek et al. 2013):

$$\begin{aligned} \frac{\partial \theta C_k}{\partial t} + \rho \frac{\partial S_k}{\partial t} + a_v \frac{\partial g_k}{\partial t} \\ = \frac{\partial}{\partial z} \left( \theta D_i^w \frac{\partial C_k}{\partial z} \right) + \frac{\partial}{\partial z} \left( a_v D_i^g \frac{\partial C_k}{\partial z} \right) - \frac{\partial q_i C_k}{\partial z} \\ - \mu_{w,k} \theta c_k - \mu_{s,k} \rho S_k - \mu_{g,k} a_v g_k + \mu_{w,k-1} \theta c_{k-1} \\ + \mu_{s,k-1} \rho S_{k-1} + \mu_{g,k-1} a_v g_{k-1} k \epsilon (2, n_s), \end{aligned}$$



where  $C$ ,  $S$  and  $g$  are dissolved ( $\text{ML}^{-3}$ ), solid ( $\text{MM}^{-1}$ ) and gaseous phase ( $\text{ML}^{-3}$ ) concentrations respectively,  $\rho$  is the bulk density ( $\text{ML}^{-3}$ ),  $z$  is spatial coordinate (L),  $D_{iw}$  and  $D_{ig}$  are the effective dispersion tensor for the dissolved and gaseous phases ( $\text{L}^2\text{T}^{-1}$ ),  $q$  is volumetric flux density ( $\text{LT}^{-1}$ ),  $\mu_w$ ,  $\mu_s$  and  $\mu_g$  are the first-order decay constants for the liquid, solid and gaseous phases ( $\text{T}^{-1}$ ), respectively. These constants are connected between each individual species in the chain, with  $k$  being the ordinal number and  $n$  being the number of solutes in the chain.

Urea ( $\text{CO}(\text{NH}_2)_2$ ) is hydrolyzed by heterotrophic bacteria after its placement in the soil to form ammonium ion ( $\text{N-NH}_4$ ). According to soil pH and temperature,  $\text{N-NH}_4$  can be transform to  $\text{N-NH}_3(g)$  and be lost to the atmosphere (Kissel et al. 2008). The dissolved phase ( $C$ ) was considered in equilibrium with the gaseous phase ( $g$ ) according to Henry's law:

$$g = C \times K_h,$$

where  $K_h$  is the Henry's constant.

$\text{N-NH}_4$  is usually absorbed to solid components of the soil, diminishing its leaching potential. The adsorption process was considered as an instantaneous process between soil solution and interchangeable sites, and could be express in its linear form as:

$$S = C \times K_d,$$

where  $K_d$  is the soil–water partitioning coefficient.

The remaining ammonium in soil is transformed under aerobic conditions by the action bacteria in two steps, first to nitrites (by *Nitrosomas*) and then to nitrates (by *Nitrobacter*). Nitrites are an intermediate product, and its formation reaction is generally much faster than nitrification of ammonia (Hanson et al. 2006). The final product of the decay chain of urea is nitrate ( $\text{N-NO}_3$ ), which is not retained by solid particles and presents great leachate potential. The solute transport parameters used in the simulations (Table 2) were taken as the mean values used in the bibliography for agronomic soils. The hydrolysis first-order decay constant is normally

between the range of  $0.2\text{--}0.56 \text{ day}^{-1}$  (Eltarabily et al. 2019; Shafeeq et al. 2020). Nitrification of ammonium to nitrites and then nitrates was couple into one unique reaction using the rate constant:  $0.2 \text{ day}^{-1}$ . Values for nitrification showed in the literature are very diverse, being  $0.2 \text{ day}^{-1}$  (Hanson et al. 2006; Akbariyeh et al. 2018),  $0.02\text{--}0.5 \text{ day}^{-1}$  (Lotse et al. 1992) and from  $0.4$  to  $0.6 \text{ day}^{-1}$  (Shafeeq et al. 2020). Denitrification process was not accounted, as it can be considered negligent under aerated conditions (Gärdenäs et al. 2005). As the objective of this study was to determine the influence of climate conditions over nitrogen compounds transport rate, the reactions parameters were fixed constant during the simulated time (100 years) and under the different climate-change scenarios.

### 2.4.3 Domain Properties and Boundary Conditions

Water flow was simulated in a one-dimension vertical profile of 100 cm deep. Simulations were made on a daily time scale for 100 years (36,500 days). The time discretization (days) was as follows: initial time step 0.001, minimum time step  $1\text{E-}5$  and maximum time step 5. Soil hydraulic parameters were estimated based on Rosseta pedotransfer function (Schaap et al. 2001) for a sandy loam texture. An atmospheric boundary condition was considered for the upper boundary and a free drainage boundary condition for the lower boundary. Daily precipitation and potential evapotranspiration were introduced into the model according to each climate-change scenario. The reference evapotranspiration ( $\text{ET}_0$ ) was calculated based on Hargreaves method (Hargreaves and Samani 1985) according to the minimum and maximum air temperature. The crop evapotranspiration ( $\text{ET}_c$ ) was calculated based on the single crop coefficient ( $K_c$ ) (Allen et al. 1998):

$$\text{ET}_c = \text{ET}_0 \times K_c,$$

where  $K_c$  was taken as 0.75 for extensive grazing pastures at middle-end growing season. The effect of both crop transpiration and soil evaporation are integrated into a single crop coefficient.

**Table 2** Solute transport parameters used in the numerical modeling

Solute	$K_d$ ( $\text{L kg}^{-1}$ )	$K_h$ (–)	$\mu_h$ ( $\text{day}^{-1}$ )	$\mu_n$ ( $\text{day}^{-1}$ )	$D_w$ ( $\text{cm}^2 \text{ day}^{-1}$ )	$D_g$ ( $\text{cm}^2 \text{ day}^{-1}$ )
Urea–N	–	–	0.38 <sup>a</sup>	–	1.52 <sup>b</sup>	–
$\text{N-NH}_4$	3.5 <sup>a</sup>	0.000295 <sup>b</sup>	–	0.2 <sup>a</sup>	1.52 <sup>b</sup>	18,057.6 <sup>b</sup>
$\text{N-NO}_3$	–	–	–	–	1.64 <sup>b</sup>	–

$K_d$  soil–water partitioning coefficient,  $K_h$  Henry's constant,  $\mu_h$  hydrolysis first-order decay constant,  $\mu_n$  nitrification first-order decay constant,  $D_w$  molecular diffusion coefficient in free water,  $D_g$  molecular diffusion coefficient in soil air

<sup>a</sup>Hanson et al. (2006)

<sup>b</sup>Li et al. (2015)

For solutes transport, boundary conditions were assumed as Cauchy type or third type. This condition is used to prescribe the concentration flux along a boundary segment (Šimůnek et al. 2013). To compare different climate scenarios effect over urea and N compounds fate, only one fertilization schedule was incorporated into the model. The reference input of urea (46% N) was assumed as  $33 \text{ kg N Ha}^{-1} \text{ year}^{-1}$ . Solute was considered to enter the soil dissolved in a sheet of water of 10 mm ( $C=0.33 \text{ mg N cm}^{-3}$ ). The numerical model did not account solute extraction by roots. This fact could be justified as this amount of N corresponds to the excess of total N applied with respect to the need of any crop under inappropriate soil management. Wang et al. (2019) informed that the global use of N fertilizer input for various crop from 46 countries is around  $109 \text{ kg N Ha}^{-1} \text{ year}^{-1}$ . The current global mean N leaching derived from synthetic fertilizer is calculated as 30% by the IPCC (IPCC 2006).

## 2.5 Statistical Analysis

The relationship between variations in the output variables and climate change were analyzed based on the Pearson correlation coefficient ( $r$ ). This statistical index, ranges from  $-1$  to  $1$ , where positive values indicate similar trends between variables while negative values indicate an opposite behavior. The correlation was statistically significant only if the  $p$  value was lower than the significance level (e.g., 0.01). The data set involved the mean monthly change for each variable at the end of the twenty-first century with respect to the reference period (RCP0.0) under all four climate-change scenarios. As exposed by Saadatabadi et al. (2021), the response of hydrological variables produced by precipitation or temperature change could present a lag time. So, the analysis was carried out considering both, a non-time-lagged correlation, and a time-lagged correlation (1 and 2 months).

## 3 Results and Discussion

### 3.1 Validation of Climate Setups

A synthetic climate series was created for the study area based on antecedent meteorological data. Figure 2 shows the comparison between the mean measured and predicted precipitation for each month of the year. The predicted values by the weather generator correctly represents rain conditions for the 64-year series. Although, monthly rainfall estimated by the weather generator is lower for some month of the year, the predicted yearly average precipitation differs only 3% from the measured value. Overall, rainfall distribution along the year is well characterized as the coefficient of determination ( $R^2$ ) presents a value of 0.99.

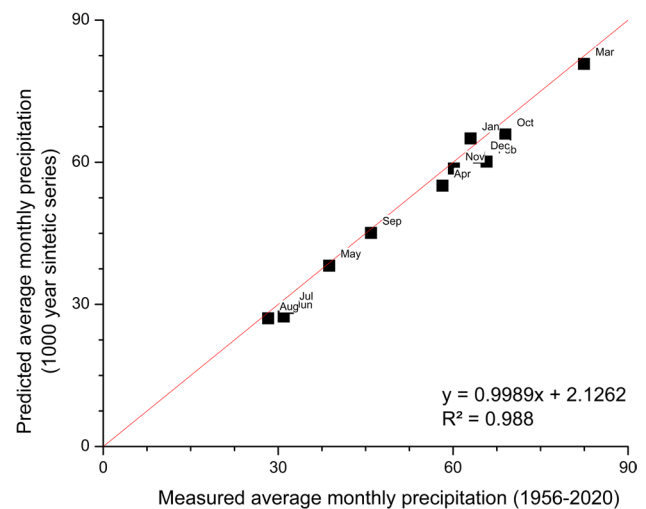
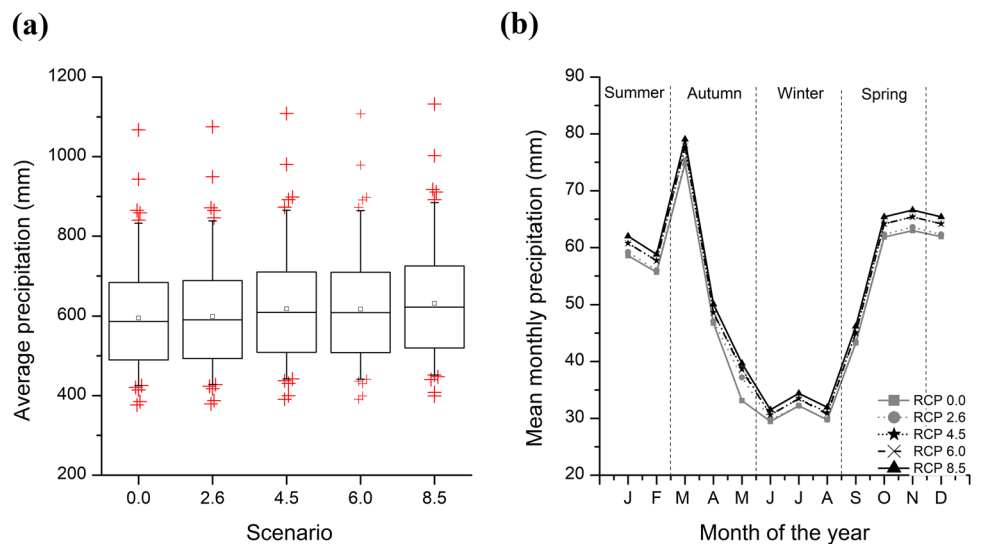


**Fig. 2** Linear fit between the measured and predicted average monthly precipitation

The new synthetic climate series was modified according to each climate-change scenario predicted by the IPCC. Figure 3 shows the predicted mean annual precipitation (Fig. 3a) and the mean monthly precipitation (Fig. 3b) for the five future climate scenarios. The climate-change scenarios correspond to the expected increase of precipitation by the end of the twenty-first century (2081–2100). The annual mean precipitation had a value of 598 mm, 617 mm, 617 mm, and 631 mm for the scenarios of RCP2.6, RCP4.5, RCP6.0 and RCP8.5, respectively. As seen in Fig. 3a, the average yearly rainfall value is always higher than the median, suggesting that the number of wet years in the series is lower than the dry years. Although high values of precipitation for these years increase the average value of the series. Extremes values, for both wet and dry years are marked as outliers in the box chart. The outliers were defined as the 5% and 95% percentile, equivalent to annual precipitation lower than 420 mm (RCP0.0)—460 mm (RCP8.5), or higher than 840 mm (RCP0.0)—870 mm (RCP8.5). Regarding the annual distribution of rainfall, the greater increases of precipitation is expected for spring and summer seasons (Fig. 3b). As these months, also corresponds to the period of higher water demand for evapotranspiration, climate change could be initially considered as a positive variation for the semiarid Pampas, as more water would be available for crops. However, precipitation increase will be also accomplished by an increase in air temperature for all seasons. Thus, it is necessary to evaluate soil water storage alongside actual evapotranspiration and deep-water drainage to asseverate this fact. Otherwise, an increase in precipitation for all scenarios could also be related to higher leachate of N in this region.

**Fig. 3** Variation in precipitation for the five climate scenarios. **a** Box-whisker plot of annual average precipitation for the 100 years considered in the simulation. The central line indicates the median; the top box edges indicate the 25th and 75th percentiles, respectively; the whiskers extend to the most extreme data points not considered outliers, and the outliers are plotted individually using the red '+' symbol. **b** Mean monthly precipitation for each climate scenario

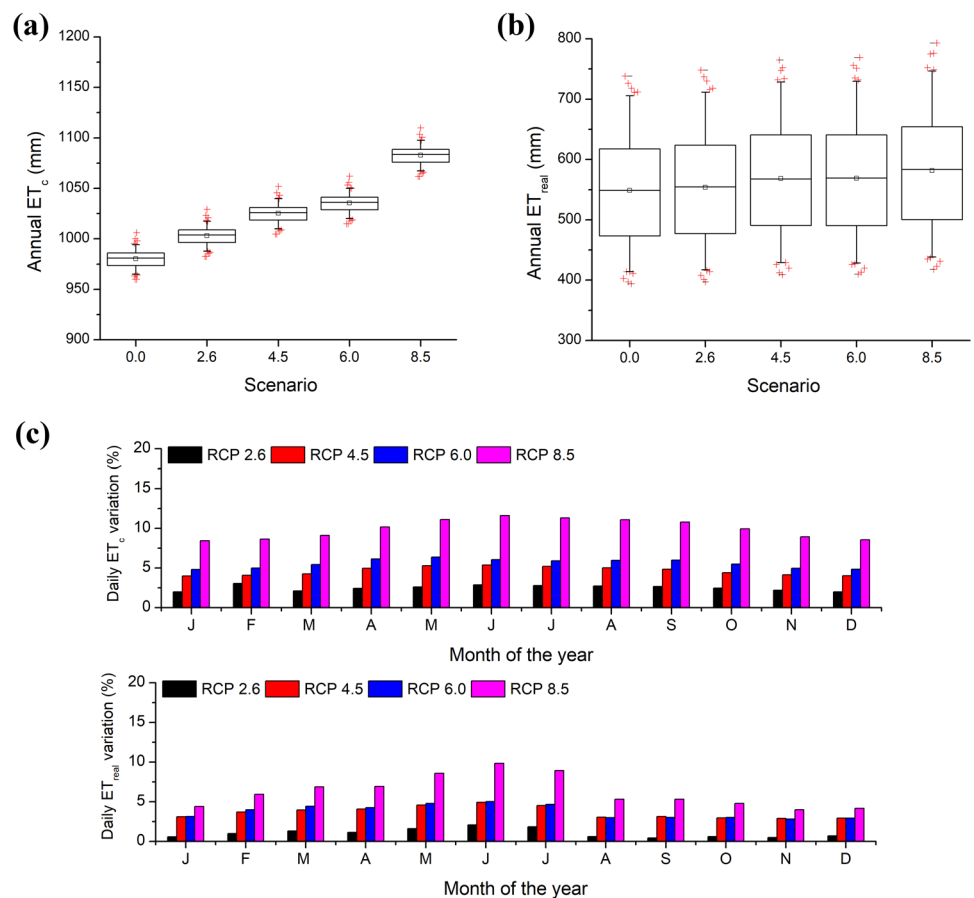


### 3.2 Potential and Actual Evapotranspiration

As stated by the IPCC (2013), in the Southeast South American region the annual temperature is expected to increase around 0.8 °C for the lowest greenhouse emissions scenario (RCP2.6) and 3.7 °C for the worst scenarios for

climate change (RCP8.5). In all cases, summer temperatures are expected to increase more than winter temperatures. Thus, annual temperature variations between seasons will be notably intensify. A rise in air temperature is expected for all month of the year, so water demand by plants and atmosphere is going to increase as well, as shown in Fig. 4a.

**Fig. 4** Evapotranspiration for each climate-change scenario. **a** Box-whisker plot of annual potential evapotranspiration for a grazing pasture. **b** Box-whisker plot of annual actual evapotranspiration according to HYDRUS 1D simulation. The central line indicates the median; the top box edges indicate the 25th and 75th percentiles, respectively; the whiskers extend to the most extreme data points not considered outliers, and the outliers are plotted individually using the red '+' symbol. **c** Percentual changes in the potential and actual evapotranspiration at the end of the twenty-first century with respect to the reference period (RCP0.0) under all four future scenarios



Calculated mean values of  $ET_c$  ranged from 980 mm under the actual climate conditions (RCP0.0) and 1083 mm under the highest temperature rise scenario (RCP8.5). For this last scenario, water demand will increase approximately 10.5%. However, an increase in precipitation is also expected for this region. Thus, the actual evapotranspiration ( $ET_{real}$ ) will also be slightly increased from 548 mm in RCP0.0 to 553 mm (+0.91%), 568 mm (+3.65%), 568 mm (+3.65%), and 581 mm (+6.02%) in RCP2.6, RCP4.5, RCP6.0 and RCP8.5 scenarios, respectively (Fig. 4b).

An increase in annual rainfall in the semiarid Pampas, could be considered as a positive variation. However, the increase in precipitation will not cover the new potential water demand by plants. Figure 4c illustrates the mean percentage change in the potential and actual evapotranspiration at the end of the twenty-first century with respect to the reference period (RCP0.0) under the four changing climates. From low to high climate-change scenarios, increases in potential evapotranspiration are greater as higher temperature raises are expected for all month of the year. Moreover, for the same scenario the variations are quite similar during all months. However, changes in actual evapotranspiration do not show a homogeneous trend throughout the year. The new atmospheric demand is mostly satisfied between April and June. Nevertheless, the increase in actual evapotranspiration during August-February is much smaller showing that water availability is not going to be equitable throughout the year.

Figure 5a shows the  $ET_{real}$  to  $ET_c$  ratio for all future climate scenarios. This ratio is a measure of plant water supply in relation to plant water requirement. According to Yao (1974), values close to 0.90 can be assumed as optimum

water requirement and values lower than 0.60 can be considered as requiring irrigation for crop growth.

Under the RCP0.0 climate conditions, the mean water demand satisfied by precipitation is around 56%, thus crop yields are limited by water availability in current climate. This condition is expected to be worse for all changing climates. Water demand by plants satisfied by rainfall is diminishing by 1.5% (RCP2.6), 1.0% (RCP4.5), 1.9% (RCP6.0) and 4.1% (RCP8.5). In semiarid region with rain-fed agriculture and livestock, variation in thermal and rainfall extremes can affect the structure of agroecosystems (Ferrelli et al. 2019). These reductions will have to be countered by irrigation or alternatively, the agricultural production could be reduced (Valdes-Abellan et al. 2020). Furthermore, water stress for crops is expected to increase more in the warmer seasons than the cooler seasons of the year as shown in Fig. 5b. For the medium to high end scenarios, the  $ET_{real}$  to  $ET_c$  ratio is expected to decline by 3–6% in spring and 2–5% in summer months. Instead, the ratio is expected to only decrease 1.5–2.2% in autumn and 1.8–2.5% in winter. According to CIMP5 projections temperature increases are higher from September to February, while precipitation variations are more important from April to September. Almazroui et al. (2021) suggest that precipitation is becoming more seasonal in the future climate for South America region, whatever of the net change. If dry periods coincide with the warmer months, the consequences on crops in the region will be worse, especially in the RCP6.0 and RCP8.5 scenarios.

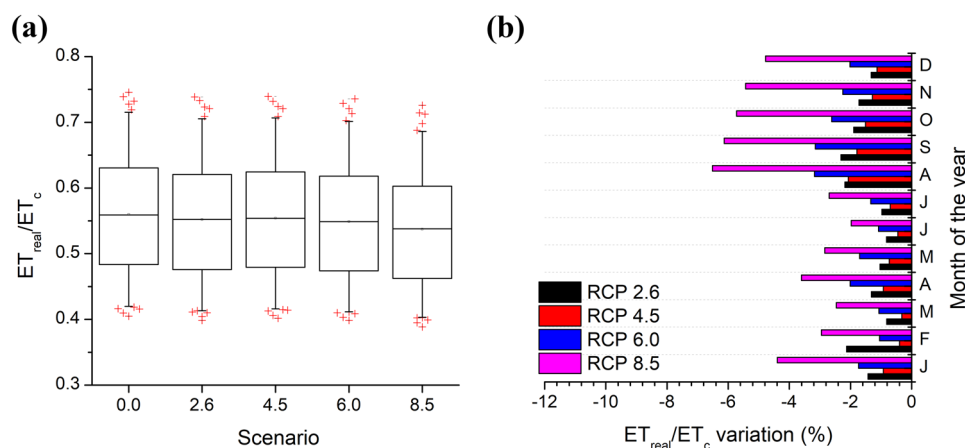
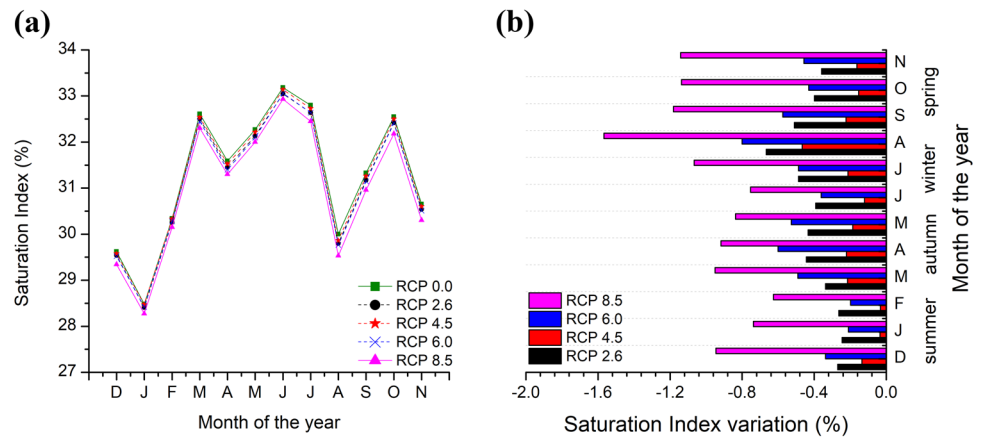


**Fig. 5** **a** Box-whisker plot of the relation between potential and actual evapotranspiration for the set of 100 years. The central line indicates the median; the top box edges indicate the 25th and 75th percentiles, respectively; the whiskers extend to the most extreme data points not

considered outliers, and the outliers are plotted individually using the red '+' symbol. **b** Percentual changes in the monthly evapotranspiration ratio at the end of the twenty-first century with respect to the reference period (RCP0.0) under all four future scenarios



**Fig. 6** **a** Mean saturation index for the topsoil (15 cm) according to HYDRUS 1D simulation. **b** Percentual variation in the saturation index at the end of the twenty-first century with respect to the reference period (RCP0.0) under all four future scenarios



### 3.3 Soil Water Storage and Deep-Water Drainage

Figure 6a shows the mean monthly saturation index for the topsoil (15 cm) simulated by HYDRUS 1D for each climate-change scenario during the 100 years series. Overall, variations in water contents for the one-meter soil profile are very limited. Soil water contents are expected to decrease for all month of the year in all changing climates. In all cases, moisture contents are higher for autumn and winter and lower for spring and summer. As explained before, evapotranspiration is greater in warmer months, thus soil water storage decreased during these seasons. The number of days where the soil is drier than the average is greater than the number of days where the soil is wetter. As the climate-change scenarios implicate a gradual increase in both, precipitation and temperature, most of the new input of water from precipitation is consumed by the evapotranspiration process. Excessive heat might dry the soil and inhibit vegetation growth (Ferrelli et al. 2021). Temperature increases

affects crops' flowering, delaying the growing season, and shortening the critical period, resulting in diminishing yields (Fernández-Long et al. 2013). However, as the increase in temperature is accompanied by an increase in precipitation, soil dryness is dampened. Figure 6b shows the percentual variation in the saturation index for the topsoil with respect to the reference period (RCP0.0) in all four future changing scenarios. It should be highlighted that the average moisture contents are expected to be lower for RCP2.6 than RCP4.5 changing scenarios. In the RCP4.5 scenario, the annual temperature increase would be only around 1.6 °C, but the increase in rainfall would reach 4%. Under this condition, soil water contents were very similar to moisture evolution according to the current climate (RCP0.0). The most significant changes corresponded to the RCP8.5 scenario where the mean monthly moisture contents may decline by 0.7–1.6% between August and December.

Similarly, the deep-water drainage present slight variations between the scenarios. The annual average value

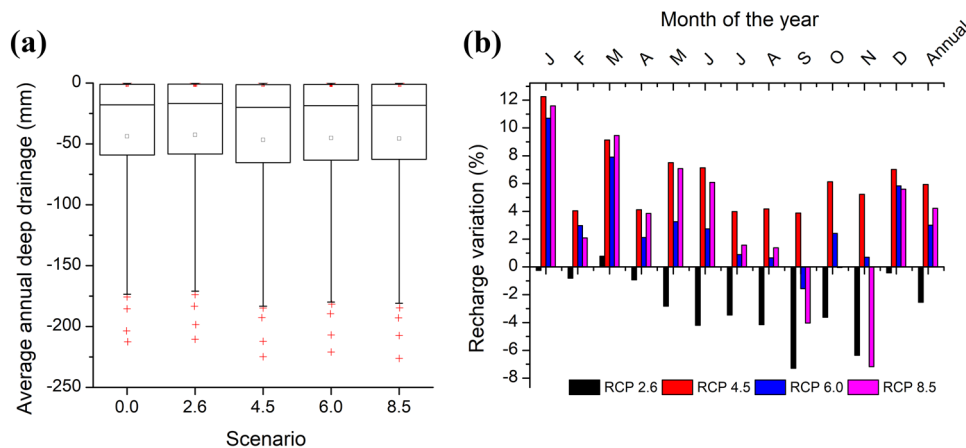


**Fig. 7** **a** Box-whisker plot of average annual deep-water drainage according to HYDRUS 1D simulation. The central line indicates the median; the top box edges indicate the 25th and 75th percentiles, respectively; the whiskers extend to the most extreme data points not

considered outliers, and the outliers are plotted individually using the red '+' symbol. **b** Percentual changes in deep drainage at the end of the twenty-first century with respect to the reference period (RCP0.0) under all four future scenarios

of deep drainage was estimated as 43.8 mm (7.36% rainfall), 42.6 mm (7.11% rainfall), 46.6 mm (7.53% rainfall), 45.2 mm (7.31% rainfall) and 45.6 mm (7.21% rainfall) for the RCP0.0, RCP2.6, RCP4.5, RCP6.0 and RCP8.5 scenarios, respectively (Fig. 7a). These values are consistent with those established by Carrica and Lexow (2004) for the study area by different hydrogeological methods. The authors estimated that recharge represents between 7 and 8.5% of precipitation under current climate conditions. Recharge plays a major role in groundwater availability, as well as in assessing the vulnerability of aquifers to contamination (Scanlon et al. 2002). Although net changes in deep drainage between scenarios are limited, important variations in the monthly components of recharge are recognized. Figure 7b shows the percentual changes in deep drainage at the end of the twenty-first century with respect to the reference period (RCP0.0) under all four future scenarios. The annual variation in deep drainage was estimated as  $-2.5\%$ ,  $+5.9\%$ ,  $+3.0\%$  and  $+4.2\%$  for low to high changing climate scenarios, respectively. The RCP2.6 scenario shows a negative variation in deep drainage for all month except March. In contrast, the rest scenarios show positive variations in recharge during most of the year. Increase in extreme events of precipitation could be linked to this process. In semiarid regions, water balance tends to be negative when expressed on annual basis. However, precipitation can exceed potential evapotranspiration in certain months of the year and net recharge may occur (Montoya et al. 2019). Beigi and Tsai (2015) found that the potential recharge rate is most sensitive to precipitation variation than temperature change comparing different climate-change scenarios for various regions of North America. The increase of recharge in medium to high

climate changing scenarios is a remarkable result. Water supply for irrigation of fields and livestock maintenance mainly comes from the exploitation of the phreatic aquifer in the semiarid region of the Pampas (Carrica and Lexow 2004; Montoya et al. 2019). Thus, the predicted increase in crop water demand could be supplied by groundwater exploitation without harming resources except for the RCP2.6 scenario.

### 3.4 N Compounds Fate

The fate of N compounds derived from the use of urea were analyzed for the five climate conditions. Nitrogen losses due to volatilization of ammonia and nitrate leachate were chosen as reference parameters to compare the impact of climate change on solute transport. Both parameters relate to economic and environmental impacts of agriculture activity. Figure 8a shows the percentual changes in ammonia volatilization at the end of the twenty-first century with respect to the reference period (RCP0.0) under all four future changing scenarios. Overall, the mean emission of  $\text{N-NH}_3$  is approximately  $4 \text{ kg N ha}^{-1}$  (12% of applied urea-N). However, slight variations are recognized in the annual amount of volatilize ammonia when comparing to the actual climate conditions. In the RCP2.6 scenario ammonia volatilization is expected to increase 0.3%. In middle to high changing scenarios, ammonia volatilization is going to decrease by 0.75% (RCP4.5), 0.43% (RCP6.0) and 0.26% (RCP8.5). Ammonia volatilization is influenced by soil properties such as soil pH, moisture, soil texture, as well as climate conditions such as air temperature, light, wind speed, and precipitation (Kissel et al. 2008). As simulations were run for the same soil profile, variations are only related to climate conditions. Small

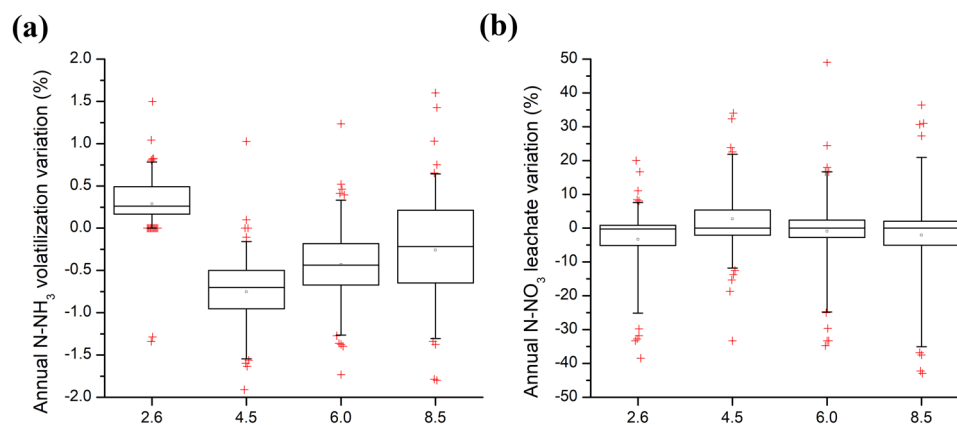


**Fig. 8** Box-whisker plot of annual solute fluxes variations according to HYDRUS 1D simulation. **a** Percentual changes in ammonia volatilization at the end of the twenty-first century with respect to the reference period (RCP0.0) under all four future scenarios. **b** Percentual changes in nitrate leachate at the end of the twenty-first century with

respect to the reference period (RCP0.0) under all four future scenarios. The central line indicates the median; the top box edges indicate the 25th and 75th percentiles, respectively; the whiskers extend to the most extreme data points not considered outliers, and the outliers are plotted individually using the red '+' symbol

differences in the volatilization rate are correlated with low moisture variations for the topsoil. According to Pelster et al. (2019), water contents directly influence ammonia volatilization. Maximum losses are expected where there is sufficient soil water to facilitate urea hydrolysis, but still enough air to allow for rapid flow. Water fills up soil micropores first, promoting preferential gas flow through macropores. As water contents increases, these larger pores are also fill, reducing gas diffusion rates.

Figure 8b shows the percentual variation in nitrate leachate at the end of the twenty-first century with respect to the reference period (RCP0.0) under all four future scenarios. The greater average value of N-NO<sub>3</sub> leachate corresponds to the RCP4.5 scenario, being approximately 86.18% of total applied urea-N. This amount represents an increase of 2.8% respect to the actual climate conditions. In the RCP4.5 scenario, the higher value of deep-water drainage was also determined. As expected, nitrate leaching is related to soil bottom water fluxes. Groundwater vulnerability to contamination by nitrate leaching increases in medium to high climate-change scenarios. As the recharge rates increases the amounts of N transported to the aquifer will also be higher. Long and Sun (2012) suggested that monthly precipitation and nitrate leaching losses are significantly correlated. The lower amount of average N-NO<sub>3</sub> leachate corresponds to the RCP2.6 scenario. The mean annual nitrate leachate is expected to decrease by 3.3%. As shown previously this climate scenario, was the only one with a decline in recharge rates. The RCP6.0 and RCP8.5 scenarios showed the most extreme rates of change compared to the current climate. Although the mean response indicates leaching values similar to RCP0.0, there are years where both increases and decreases of up to 50% are observed. Raises in nitrate leachate could relate to the occurrence of more extreme precipitation that allow the rapid transport of nitrates to the aquifers. Contrary, dry years could be assigned to null N leaching. Nitrates accumulated in the soil during these years

could be washed off in humid years, generating leachate of much greater quantities than the annual input of urea-N to the profile.

### 3.5 Statistical Analysis

The Pearson correlation analysis was applied to establish the relationship between changes of output variables in response to precipitation and temperature variation for all changing future scenarios. Table 3 shows the statistical index calculated for the non-time-lagged correlation and the time-lagged correlations (one and two months). The relationship between precipitation and the reference evapotranspiration (ET<sub>c</sub>) was not calculated as the last one only depends on temperature. Precipitation showed a significant positive correlation with ET<sub>real</sub> and deep drainage. In the first case, the highest Pearson correlation coefficient (*r*) was obtained for the non-time-lagged correlation. Instead, deep drainage showed an improvement of “*r*” in the time-lagged correlation with a 2-month delay. This may relate to the time required for percolating water to reach the bottom boundary of soil profile. According to Nazarieh et al. (2018) the lag time depends on factors such as soil hydraulic conductivity, vadose zone depth, percolation rates and the antecedent soil-moisture condition. Temperature showed a significant positive correlation with ET<sub>c</sub> and ET<sub>real</sub>. Otherwise, the relationship between temperature and soil saturation index was significantly negative correlated. Temperature always presented the highest “*r*” values for the non-time-lagged correlation, suggesting that hydrological changes produced by this variable have no delay in its response. Solute transport variables as volatilization and lixiviation were not significantly correlated with precipitation or temperature change. In addition to climatic variables, the magnitude of these processes could be also affected by factors such as the time and rate of fertilizer application and the degradation rate of nitrogen compounds, which were not considered in this study.

**Table 3** Pearson correlation analysis between variations in each variable and climate change (precipitation and temperature)

	ET <sub>c</sub>	ET <sub>real</sub>	Saturation index	Deep drainage	N volatilization	N lixiviation
Non-time-lagged correlation						
Precipitation	–	0.899**	– 0.508**	0.393**	– 0.304	– 0.012
Temperature	0.777**	0.902**	– 0.749**	0.285	– 0.193	– 0.032
Time-lagged correlation (1 month)						
Precipitation	–	0.784**	– 0.472**	0.345	– 0.198	0.013
Temperature	0.742**	0.872**	– 0.738**	0.317	– 0.112	0.007
Time-lagged correlation (2 months)						
Precipitation	–	0.785**	– 0.371**	0.511**	– 0.325	0.319
Temperature	0.722**	0.862**	– 0.730**	0.331	– 0.146	0.034

\*\*Correlation is significant at the 0.01 level

## 4 Conclusions

Climate change scenarios predicted for the southeast South American region at the end of the twenty-first century indicate a slight increase of precipitation and air temperatures. Simulations carried out with HYDRUS 1D software were used to compare the evolution of soil water fluxes and nitrogen fate derived from urea fertilizer under five different climate-change scenarios.

According to our results, the mean annual actual evapotranspiration is going to increase between 1 to 6% from low to high climate-change scenarios. Although an increase in precipitation is expected during all months of the year, there are periods when water availability will not be enough to supply the new potential evapotranspiration demand. Thus, an increase in water stress for crops is expected for the region. The most unfavorable case is the RCP8.5 scenario where the  $ET_{\text{real}}/ET_c$  ratio decreases by 4%. The warmer seasons showed higher increases in the water stress index than the colder seasons. If dry seasons coincides with the warmer months, the consequences on crops will be aggravated, especially in the cases of RCP6.0 and RCP8.5 scenarios.

Although variations in the average soil-moisture content are subtle, a decrease is expected during all months of the year for all scenarios. The lowest decline is recorded for the RCP4.5 scenario, while the highest drop is expected for the RCP8.5 scenario. In relation to deep drainage, a decrease in annual recharge of 2.5% is expected in the RCP2.6 scenario, while in the rest of the scenarios the potential annual recharge would increase by 5.9% (RCP4.5), 3.0% (RCP6.0) and 4.2% (RCP8.5). The increase in recharge in the most drastic scenarios is a positive modification for the region, given the dependence of agricultural and livestock activities on groundwater resources.

Regarding the fate of N compounds derived from urea fertilizer, N losses due to volatilization were around 12% of the total N applied in all cases. In the RCP2.6 scenario ammonia volatilization is expected to increase 0.3%. In middle to high changing scenarios, ammonia volatilization is going to decrease by 0.75% (RCP4.5), 0.43% (RCP6.0) and 0.26% (RCP8.5). Nitrogen leachate in the form of nitrates showed an increase of 2.8% in the RCP4.5 scenario, which was the one with the highest recharge rates raises. Although the net change of nitrate leachate for the RCP6.0 and RCP8.5 scenarios was similar to RCP0.0, these showed the greatest dispersion potentially related to the occurrence of extreme climate conditions. More specific studies should be made on the effect of temperature increase on the biochemical reactions of nitrogen compounds in soil.

The methodology applied in the present work could be adapted to other regions of the world. The use of a mathematical model as a predictive tool in soil water fluxes and fertilizers use is essential for planning the sustainable management of soil adapted to climate changes. Results obtained in this work will be useful to stakeholders and decision-makers to orientate agroecological management from semi-arid regions.

**Acknowledgements** This research is financially supported by the Universidad Nacional del Sur (UNS) and Consejo Nacional de Investigaciones Científicas y Técnicas (CONICET).

**Author contributions** LES and JV-A contributed to the conception and design of the study. Material preparation, data collection and analysis were performed by LES, JV-A and VZ. Software simulations were performed by LES and JV-A. The first draft of the manuscript was written by LES, JV-A, and VZ. Funding and resources were managed by LC. All authors commented on previous versions of the manuscript. All authors read and approved the final manuscript.

**Funding** This research is financially supported by the Universidad Nacional del Sur (UNS) and Consejo Nacional de Investigaciones Científicas y Técnicas (CONICET).

**Availability of data and material** The datasets generated during and/or analyzed during the current study are available from the corresponding author on reasonable request.

**Code availability** Not applicable.

## Declarations

**Conflict of interest** The authors have no relevant financial or non-financial interests to disclose.

**Ethics approval** The authors declare that the manuscript complies with the ethical rules applicable to this journal.

**Consent to participate** Not applicable.

**Consent for publication** All authors give their consent to publish this work.

## References

- Abera K, Crespo O, Seid J, Mequanent F (2018) Simulating the impact of climate change on maize production in Ethiopia, East Africa. *Environ Syst Res*. <https://doi.org/10.1186/s40068-018-0107-z>
- Abraham EM, Guevara JC, Candia RJ, Soria ND (2016) Dust storms, drought and desertification in the Southwest of Buenos Aires Province, Argentina. *Rev La Fac Ciencias Agrar UNCuyo* 48:221–241
- Akbariyeh S, Bartelt-Hunt S, Snow D et al (2018) Three-dimensional modeling of nitrate–N transport in vadose zone: roles of soil heterogeneity and groundwater flux. *J Contam Hydrol* 211:15–25. <https://doi.org/10.1016/j.jconhyd.2018.02.005>



- Allen RG, Pereira LS, Raes D, Smith M (1998) FAO irrigation and drainage paper no. 56: Crop Evapotranspiration
- Almazroui M, Ashfaq M, Islam MN et al (2021) Assessment of CMIP6 performance and projected temperature and precipitation changes over South America. *Earth Syst Environ* 5:155–183. <https://doi.org/10.1007/s41748-021-00233-6>
- Amiotti N, Blanco MC, Sanchez LF (2001) Complex pedogenesis related to differential aeolian sedimentation in microenvironments of the southern part of the semiarid region of Argentina. *CATENA* 43:137–156. [https://doi.org/10.1016/S0341-8162\(00\)00126-0](https://doi.org/10.1016/S0341-8162(00)00126-0)
- Barbieri PA, Rozas HS, Echeverría HE (2008) Time of nitrogen application affects nitrogen use efficiency of wheat in the humid pampas of Argentina. *Can J Plant Sci* 88:849–857. <https://doi.org/10.4141/CJPS07026>
- Barros VR, Doyle ME, Camilloni IA (2008) Precipitation trends in southeastern South America: relationship with ENSO phases and with low-level circulation. *Theor Appl Climatol* 93:19–33. <https://doi.org/10.1007/s00704-007-0329-x>
- Barros VR, Boninsegna JA, Camilloni IA et al (2015) Climate change in Argentina: trends, projections, impacts and adaptation. *Wiley Interdiscip Rev Clim Chang* 6:151–169. <https://doi.org/10.1002/wcc.316>
- Barros V, Castañeda ME, Doyle M (2000) Recent precipitation trends in southern South America east of the Andes: an indication of climatic variability. In: *Southern hemisphere paleo-and neoclimates*. Springer, pp 187–206
- Beigi E, Tsai FTC (2015) Comparative study of climate-change scenarios on groundwater recharge, southwestern Mississippi and southeastern Louisiana, USA. *Hydrogeol J* 23(4):789–806. <https://doi.org/10.1007/s10040-014-1228-8>
- Cabré MF, Solman S, Núñez M (2016) Regional climate change scenarios over southern South America for future climate (2080–2099) using the MM5 model. Mean, interannual variability and uncertainties. *Atmosfera* 29:35–60. <https://doi.org/10.20937/ATM.2016.29.01.04>
- Carbonetto B, Rascovan N, Álvarez R et al (2014) Structure, composition and metagenomic profile of soil microbiomes associated to agricultural land use and tillage systems in Argentine Pampas. *PLoS ONE*. <https://doi.org/10.1371/journal.pone.0099949>
- Carrica JC, Lexow C (2004) Evaluación de la recarga natural al acuífero de la cuenca superior del arroyo Napostá Grande, provincia de Buenos Aires. *Rev La Asoc Geol Argentina* 59:281–290
- Díaz-Zorita M, Duarte GA, Grove JH (2002) A review of no-till systems and soil management for sustainable crop production in the subhumid and semiarid Pampas of Argentina. *Soil Tillage Res* 65:1–18. [https://doi.org/10.1016/S0167-1987\(01\)00274-4](https://doi.org/10.1016/S0167-1987(01)00274-4)
- Eltarabily MG, Bali KM, Negm AM, Yoshimura C (2019) Evaluation of root water uptake and urea fertigation distribution under sub-surface drip irrigation. *Water (switzerland)* 11:1–15. <https://doi.org/10.3390/w11071487>
- Feddes RA, Bresler E, Neuman SP (1974) Field test of a modified numerical model for water uptake by root systems. *Water Resour Res* 10:1199–1206. <https://doi.org/10.1029/WR010i006p01199>
- Ferm M (1998) Atmospheric ammonia and ammonium transport in Europe and critical loads: a review. *Nutr Cycl Agroecosyst* 51:5–17. <https://doi.org/10.1023/A:1009780030477>
- Fernández-Long ME, Müller GV, Beltrán-Przekurat A, Scarpati OE (2013) Long-term and recent changes in temperature-based agroclimatic indices in Argentina. *Int J Climatol* 33:1673–1686. <https://doi.org/10.1002/joc.3541>
- Ferreira N, H. Miranda J, Cooke R. (2021) Climate change and extreme events on drainage systems: numerical simulation of soil water in corn crops in Illinois (USA). *Int J Biometeorol*. <https://doi.org/10.1007/s00484-021-02081-5>
- Ferrelli F, Brendel AS, Aliaga VS et al (2019) Climate regionalization and trends based on daily temperature and precipitation extremes in the south of the Pampas (Argentina). *Geogr Res Lett* 45:393–416. <https://doi.org/10.18172/cig.3707>
- Ferrelli F, Brendel AS, Perillo GME, Piccolo MC (2021) Warming signals emerging from the analysis of daily changes in extreme temperature events over Pampas (Argentina). *Environ Earth Sci*. <https://doi.org/10.1007/s12665-021-09721-4>
- Gärdenäs AI, Hopmans JW, Hanson BR, Šimůnek J (2005) Two-dimensional modeling of nitrate leaching for various fertigation scenarios under micro-irrigation. *Agric Water Manag* 74:219–242. <https://doi.org/10.1016/j.agwat.2004.11.011>
- Ghahramani A, Moore AD (2016) Impact of climate changes on existing crop-livestock farming systems. *Agric Syst* 146:142–155. <https://doi.org/10.1016/j.agry.2016.05.011>
- Greve P, Kahil T, Mochizuki J et al (2018) Global assessment of water challenges under uncertainty in water scarcity projections. *Nat Sustain* 1:486–494
- Haj-Amor Z, Bouri S (2020) Use of HYDRUS-1D–GIS tool for evaluating effects of climate changes on soil salinization and irrigation management. *Arch Agron Soil Sci* 66:193–207. <https://doi.org/10.1080/03650340.2019.1608438>
- Hanson BR, Šimůnek J, Hopmans JW (2006) Evaluation of urea–ammonium–nitrate fertigation with drip irrigation using numerical modeling. *Agric Water Manag* 86:102–113. <https://doi.org/10.1016/j.agwat.2006.06.013>
- Hargreaves GH, Samani ZA (1985) Reference crop evapotranspiration from temperature. *Appl Eng Agric* 1:96–99
- Henry B, Eckard R, Beauchemin K (2018) Review: adaptation of ruminant livestock production systems to climate changes. *Animal* 12(S2):S445–S456. <https://doi.org/10.1017/S1751731118001301>
- IPCC (2006) Guidelines for national greenhouse gas inventories – A primer, prepared by the national greenhouse gas inventories programme. IGES, Japan
- IPCC (2013) Climate change 2013: The physical science basis. Contribution of working group I to the fifth assessment report of the intergovernmental panel on climate change. Cambridge university press, Cambridge, United kingdom and New York, NY, USA
- IPCC (2014) Climate change 2014: Impacts, adaptation, and vulnerability. Part A: global and sectoral Aspects. Contribution of working Group II to the Fifth assessment report of the intergovernmental panel on climate change. Cambridge university press, Cambridge, United kingdom and New York, NY, USA
- Iqbal S, Guber AK, Khan HZ (2016) Estimating nitrogen leaching losses after compost application in furrow irrigated soils of Pakistan using HYDRUS-2D software. *Agric Water Manag* 168:85–95. <https://doi.org/10.1016/j.agwat.2016.01.019>
- Karandish F, Šimůnek J (2017) Two-dimensional modeling of nitrogen and water dynamics for various N-managed water-saving irrigation strategies using HYDRUS. *Agric Water Manag* 193:174–190. <https://doi.org/10.1016/j.agwat.2017.07.023>
- Kharin VV, Zwiers FW, Zhang X, Wehner M (2013) Changes in temperature and precipitation extremes in the CMIP5 ensemble. *Clim Change* 119:345–357. <https://doi.org/10.1007/s10584-013-0705-8>
- Kissel DE, Cabrera ML, Paramasivan M (2008) Ammonium, ammonia, and urea. *Nitrogen Agric Syst* 49:1–55
- Li Y, Šimůnek J, Zhang Z et al (2015) Evaluation of nitrogen balance in a direct-seeded-rice field experiment using Hydrus-1D. *Agric Water Manag* 148:213–222. <https://doi.org/10.1016/j.agwat.2014.10.010>
- Long GQ, Sun B (2012) Nitrogen leaching under corn cultivation stabilized after four years application of pig manure to red soil in subtropical China. *Agric Ecosyst Environ* 146:73–80. <https://doi.org/10.1016/j.agee.2011.10.013>
- Lotse EG, Jabro JD, Simmons KE, Baker DE (1992) Simulation of nitrogen dynamics and leaching from arable soils. *J Contam*



- Hydrol 10:183–196. [https://doi.org/10.1016/0169-7722\(92\)90060-R](https://doi.org/10.1016/0169-7722(92)90060-R)
- Montoya JC, Porfiri C, Roberto ZE, Viglizzo EF (2019) Assessing the vulnerability of groundwater resources in semiarid lands of central Argentina. *Sustain Water Resour Manag* 5:1419–1434. <https://doi.org/10.1007/s40899-018-0246-4>
- Morales I, Cooper J, Amador JA, Boving TB (2016) Modeling nitrogen losses in conventional and advanced soil-based onsite wastewater treatment systems under current and changing climate conditions. *PLoS ONE* 11:1–25. <https://doi.org/10.1371/journal.pone.0158292>
- Mualem Y (1976) A new model for predicting the hydraulic conductivity of unsaturated porous media. *Water Resour Res* 12:513–522. <https://doi.org/10.1029/WR012i003p00513>
- Nazariéh F, Ansari H, Ziaei AN, Izady A, Davari K, Brunner P (2018) Spatial and temporal dynamics of deep percolation, lag time and recharge in an irrigated semi-arid region. *Hydrogeol J* 26(7):2507–2520. <https://doi.org/10.1007/s10040-018-1789-z>
- Nicks AD, Lane LJ, Gander GA (1995) Weather generator. Chapter 2. USDA Water Eros Predict Proj Hillslope Profile Watershed Model Doc NSERL Rep
- Noellemeyer E, Quiroga AR, Estelrich D (2006) Soil quality in three range soils of the semi-arid Pampa of Argentina. *J Arid Environ* 65:142–155. <https://doi.org/10.1016/j.jaridenv.2005.07.007>
- Pelster DE, Watt D, Strachan IB et al (2019) Effects of initial soil moisture, clod size, and clay content on ammonia volatilization after subsurface band application of urea. *J Environ Qual* 48:549–558. <https://doi.org/10.2134/jeq2018.09.0344>
- Phogat V, Skewes MA, Cox JW et al (2014) Seasonal simulation of water, salinity and nitrate dynamics under drip irrigated mandarin (*Citrus reticulata*) and assessing management options for drainage and nitrate leaching. *J Hydrol* 513:504–516. <https://doi.org/10.1016/j.jhydrol.2014.04.008>
- Podestá G, Bert F, Rajagopalan B et al (2009) Decadal climate variability in the Argentine Pampas: regional impacts of plausible climate scenarios on agricultural systems. *Clim Res* 40:199–210
- Quiroga AR, Buschiazio DE, Peinemann N (1999) Soil compaction is related to management practices in the semi-arid Argentine Pampas. *Soil Tillage Res* 52:21–28. [https://doi.org/10.1016/S0167-1987\(99\)00049-5](https://doi.org/10.1016/S0167-1987(99)00049-5)
- Rao AVMS, Shanker AK, Rao VUM et al (2016) Predicting irrigated and rainfed rice yield under projected climate change scenarios in the eastern Region of India. *Environ Model Assess* 21:17–30. <https://doi.org/10.1007/s10666-015-9462-6>
- Rimski-Korsakov H, Alvarez CR, Lavado RS (2015) Cover crops in the agricultural systems of the Argentine Pampas. *J Soil Water Conserv* 70:134A–140A. <https://doi.org/10.2489/jswc.70.6.134A>
- Saadatabadi AR, Izadi N, Karakani EG, Fattahi E, Shamsipour AA (2021) Investigating relationship between soil moisture, hydroclimatic parameters, vegetation, and climate change impacts in a semi-arid basin in Iran. *Arab J Geosci* 14(17):1–18. <https://doi.org/10.1007/s12517-021-07831-8>
- Saadi Z, Maslouhí AM (2003) Modeling nitrogen dynamics in unsaturated soils for evaluating nitrate contamination of the Mnasra groundwater. *Adv Environ Res* (4):803–823. [https://doi.org/10.1016/S1093-0191\(02\)00055-2](https://doi.org/10.1016/S1093-0191(02)00055-2)
- Scanlon BR, Healy RW, Cook PG (2002) Choosing appropriate techniques for quantifying groundwater recharge. *Hydrogeol J* 10(1):18–39
- Schaap MG, Leij FJ, Van Genuchten MT (2001) Rosetta: a computer program for estimating soil hydraulic parameters with hierarchical pedotransfer functions. *J Hydrol* 251:163–176. [https://doi.org/10.1016/S0022-1694\(01\)00466-8](https://doi.org/10.1016/S0022-1694(01)00466-8)
- Scherger LE, Zanello V, Lexow C (2021) Impact of urea and ammoniacal nitrogen wastewaters on soil: field study in a fertilizer industry (Bahía Blanca, Argentina). *Bull Environ Contam Toxicol* 107:565–573. <https://doi.org/10.1007/s00128-021-03280-x>
- Schmidt ES, Villamil MB, Amiotti NM (2018) Soil quality under conservation practices on farm operations of the southern semiarid pampas region of Argentina. *Soil Tillage Res* 176:85–94. <https://doi.org/10.1016/j.still.2017.11.001>
- Shafeeq PM, Aggarwal P, Krishnan P et al (2020) Modeling the temporal distribution of water, ammonium–N, and nitrate–N in the root zone of wheat using HYDRUS-2D under conservation agriculture. *Environ Sci Pollut Res* 27:2197–2216. <https://doi.org/10.1007/s11356-019-06642-5>
- Šimůnek J, M. Šejna A, Saito H et al (2013) The HYDRUS-1D software package for simulating the movement of water, heat, and multiple solutes in variably saturated media, version 4.17. *HYDRUS Softw Ser* 3D 343
- Studdert GA, Echeverría HE (2000) Crop rotations and nitrogen fertilization to manage soil organic carbon dynamics. *Soil Sci Soc Am J* 64:1496–1503. <https://doi.org/10.2136/sssaj2000.6441496x>
- Valdes-Abellan J, Pardo MA, Jodar-Abellan A et al (2020) Climate change impact on karstic aquifer hydrodynamics in southern Europe semi-arid region using the KAGIS model. *Sci Total Environ* 723:138110. <https://doi.org/10.1016/j.scitotenv.2020.138110>
- van Genuchten MT (1980) A closed-form equation for predicting the hydraulic conductivity of unsaturated soils. *Soil Sci Soc Am J* 44:892–898. <https://doi.org/10.2136/sssaj1980.03615995004400050002x>
- Wang Y, Ying H, Yin Y et al (2019) Estimating soil nitrate leaching of nitrogen fertilizer from global meta-analysis. *Sci Total Environ* 657:96–102. <https://doi.org/10.1016/j.scitotenv.2018.12.029>
- Wang X, Li Y, Chen X et al (2021) Projection of the climate change effects on soil water dynamics of summer maize grown in water repellent soils using APSIM and HYDRUS-1D models. *Comput Electron Agric*. <https://doi.org/10.1016/j.compag.2021.106142>
- Wesseling JG (1991) Meerjarige simulatie van grondwaterstroming voor verschillende bodemprofielen, grondwatertrappen en gewassen met het model SWATRE. *Rapp* 152, Star Centrum, Wageningen 1–63
- Yao AY (1974) Agricultural potential estimated from the ratio of actual to potential evapotranspiration. *Agric Meteorol* 13(3):405–417. [https://doi.org/10.1016/0002-1571\(74\)90081-8](https://doi.org/10.1016/0002-1571(74)90081-8)
- Zhou ZB, Xi JG, Chen ZJ, Li SX (2006) Leaching and transformation of nitrogen fertilizers in soil after application of N with irrigation: a soil column method. *Pedosphere* 16:245–252. [https://doi.org/10.1016/S1002-0160\(06\)60050-7](https://doi.org/10.1016/S1002-0160(06)60050-7)
- Zupanc V, Šturm M, Lojen S et al (2011) Nitrate leaching under vegetable field above a shallow aquifer in Slovenia. *Agric Ecosyst Environ* 144:167–174. <https://doi.org/10.1016/j.agee.2011.08.014>